JOURNAL OF SPACECRAFT AND ROCKETS
Vol. 45, No. 5, September–October 2008

Bow Shock Wave Mitigation by Laser-Plasma Energy Addition in Hypersonic Flow

A. C. Oliveira*
Instituto Nacional de Pesquisas Espaciais, 12630-000 Cachoeira Paulista, Brazil
M. A. S. Minucci,† P. G. P. Toro,‡ and J. B. Chanes, Jr.§
Instituto de Estudos Avançados, 12228-001 São José dos Campos, Brazil
and
L. N. Myrabo¶ and H. T. Nagamatsu**
Rensselaer Polytechnic Institute, Troy, New York 12180-3590

DOI: 10.2514/1.33933

Experimental results of bow shock wave mitigation by laser-plasma energy addition in a low-density Mach 7 hypersonic flow conducted in a shock tunnel are presented. A high-power pulsed CO_2 laser operating with 7 J of energy and 30 MW of peak power was used to generate the plasma ahead of a hemispherical model installed in the tunnel test section. The schlieren technique was used to visualize the time evolution of energy addition to the flow by laser-induced plasma and the interaction between this disturbed region and the inherent bow shock formed on the model by hypersonic flow. A complete mitigation of the bow shock profile under action of the energy addition was observed. The impact pressure on the hemispherical model measured at the stagnation point reveals the correlation between the schlieren images and the pressure reduction.

I. Introduction

THE domain of the technology of hypersonic flights involves the resolution of various technological problems and requires a high degree of knowledge of interdisciplinary areas such as fluid mechanics, aerodynamics, computational fluid dynamics, lasers, plasma, and physics of new high-temperature materials. The development of airbreathing hypersonic cruiser vehicles for intercontinental transport of passengers and cargo or for lengthy military missions and the use of single-stage-to-orbit reusable vehicles to launch satellites in a more cost effective way are possible applications of such technology. The adverse conditions of a hypersonic flight environment (such as the high temperature of the vehicle leading edge, dynamic pressure load over the vehicle structure, and chemically reactive nature of the surrounding atmosphere, imposed by dissociation of N_2 and O_2 at the temperatures levels reached at hypersonic regime) are some of the challenges faced when designing hypersonic craft.

To solve part of the problems related to hypersonic and supersonic fields, a new branch of aerodynamics is being developed: plasma aerodynamics, which is plasma application as a means to control the flowfield. Among different suggestions, an interesting idea directed toward this field is the possibility of reducing the aerodynamic drag and heating of a hypersonic vehicle by adding energy to the air ahead of it. This active control of the flowfield was suggested by several authors, with different methods for its accomplishment, in which theoretical and experimental reports present the plasma generation by plasma torch [1,2], electric arcs [3,4], surface electrical discharge [5], lasers [6–10], and microwaves [11,12]. The use of a focused laser beam is an attractive solution to attain this goal [13,14]. When the optical radiation of a high-power laser is focused into a gas medium above a certain threshold, a laser-induced gas breakdown occurs and generates a spark in the focal region. The breakdown threshold depends on gas pressure, laser wavelength, optical system, and others parameters; for a pulsed CO_2 laser (IR 10.6 μm), it is over the range of 10^8–10^{10} W cm^{-2}, as shown by Hill et al. [15]. The gas inside the spark volume consists of matter in the plasma state, and the phenomenon is referred to as laser-induced optical breakdown, or laser-induced plasma. As a result, a disturbed region with lower density and higher temperature will be created upstream of the vehicle. In this scenario, the vehicle will fly in a less dense atmosphere and will experience an aerodynamic drag reduction, as well as a possible reduction of heat transfer to the vehicle surface. Because the effect of energy addition ahead of a vehicle is similar to the presence of a mechanical spike on the nose of a supersonic craft, it is referred to as a directed-energy air spike.

The analysis of the laser-induced plasma is not trivial and there is not a unique theory to explain the phenomenon as a whole; therefore, at least three approaches are presented for this purpose: the breakdown wave theory, the radiation theory, and the detonation wave theory. The reader can obtain detailed development of these theories in the work of Raizer [16,17]. To give some insight into optical gas breakdown, four stages can be distinguished in the laser-induced plasma generation: the formation of initial electron density, its growing by cascade mechanism, the plasma and detonation wave generation, and finally the blast wave and hot-gas interaction with the surrounding medium.

The air in the atmosphere and the gas used in the laboratory tests are composed of N_2, O_2, and a wide variety of contaminants such as aerosol and dust particles of several sizes. In a gaseous medium with this composition, the main mechanisms responsible for the creation of the initial electron density needed for the subsequent plasma development are multiphoton ionization and cascade-collisional ionization [inverse *bremsstrahlung* (German for decelerated radiation)]. In the first mechanism, a molecule acquires the ionization energy E_i, simultaneously absorbing n photons ($E_{\text{photon}} = h\nu$) of the incident optical radiation, obeying the condition $n = (E_i/h\nu) + 1$; the occurrence of this nonlinear optical

Received 7 August 2007; accepted for publication 4 January 2008.

*Ph.D. Candidate, Combustion and Propulsion Associated Laboratory; Research Physicist, Laboratory of Aerothermodynamics and Hypersonics; acoc@ieav.cta.br.
†Lt. Col., Brazilian Air Force, Principal Research Engineer; sala@ieav.cta.br. Senior Member AIAA.
‡Senior Research Engineer; toro@ieav.cta.br.
§Research Engineer; brosler@ieav.cta.br.
¶Associate Professor of Engineering Physics. Senior Member AIAA.
**Professor Emeritus, Mechanical Engineering, Deceased (15 May 2006).

process is very dependent on laser fluence. The bremsstrahlung is an inelastic collision mechanism in which a free electron is decelerated and emits electromagnetic radiation when colliding with an atom. Because both initial and final states of the electron in the collision are free, it is known as a free–free transition. In the inverse bremsstrahlung, however, the electron is accelerated at the collision and therefore electromagnetic energy is transformed into electron kinetic energy. Thus, after several collisions, the electron acquires high enough energy to ionize a molecule and another electron is liberated, giving rise to an avalanche multiplication of charges. After the establishment of the initial charge density, the electrons (by means of cascade ionization) quickly increase the total charge density, generating a high-temperature and high-pressure plasma. The high temperature and pressure inside the plasma volume induce the gas expansion at a velocity higher than the local sound velocity, and while the laser radiation is being absorbed, a similar mechanism of detonation wave is established; this phenomenon is referred to as a laser-supported detonation wave. At the end of the laser pulse, this mechanism ceases, the gas expansion rate decreases, and a detachment between the hot gas (core) and the shock wave occurs. The last stage is related to the energy transfer to the surroundings, in which a blast wave with decreasing velocity propagates in the medium and the hot gas equalizes the pressure with the environment and its temperature decreases while transferring energy to the cold gas.

To elucidate the effects of laser-induced plasma in hypersonic flow, the nonintrusive schlieren visualization technique [18,19] associated with a high-speed camera was adopted. The schlieren technique is based on the angular deflection undergone by a collimated light beam when passing through a medium that has a refraction index gradient. This technique is a powerful tool in hypersonic experiments because it is nonintrusive and is therefore not a source of undesirable shock waves; it is also not expensive, its alignment is not difficult, and it furnishes excellent results for shock wave visualization.

II. Experimental Apparatus

The experiments took place at the Henry T. Nagamatsu Laboratory of Aerothermodynamics and Hypersonics in Brazil. The 0.3-m Hypersonic Shock Tunnel at the Instituto de Estudos Avançados was used to produce high-, medium-, and low-enthalpy hypersonic-flow conditions [20,21]. The tests were realized with a conical nozzle with a 200-mm exit diameter and a 19.58-mm throat diameter. Depending on the reservoir temperature T_R of the shock tunnel (test gas temperature in the inlet of the nozzle), three enthalpy conditions were defined: low enthalpy if $T_R < 1000$ K, medium enthalpy if $1000\ \text{K} < T_R < 2000$ K, and high enthalpy if $T_R > 2000$ K. In the high- and medium-enthalpy runs, helium was used as the driver gas, whereas air was used in the low-enthalpy case. The useful tunnel test time depended of the enthalpy condition and varied from 400 μs for high enthalpy to 1.500 μs for low enthalpy. In the high and medium enthalpies, the tunnel was operated in the equilibrium interface condition and the reservoir conditions obtained were 4700 K and 92 bar and 1300 K and 180 bar, respectively, and in the low-enthalpy case, 930 K and 22 bar. The freestream (airflow in the test section) Mach number for these regimes was 5.6 in the high-enthalpy tests, 7.0 in the medium-enthalpy tests, and 7.3 for the low-enthalpy tests. The different Mach numbers were the result of the different reservoir conditions and real gas effects in the tests.

The facility permits experiments with the use of one pulse of a high-power CO_2 transversely excited atmospheric pressure [22] laser during the useful tunnel test time. The laser operates in the multimode regime (transversal and longitudinal) and is capable of producing a single high-energy (7.0 J) short pulse (120 ns full-width at half-maximum) at 10.6 mm. The laser-pulse profile is composed by an initial peak (120 ns) and a tail (4 μs long), with 50% of the energy in each. Therefore, when the laser operates with the maximum energy, the correspondent peak intensity is 30 MW. The output beam has a rectangular cross section of 34×17 mm, and the laser is filled with a 16:16:68 of CO_2:N_2:He gas mixture at 1-atm total pressure.

An optical mounting directs the laser beam inside the tunnel test section, as shown schematically in Fig. 1. Coupled to the test section is a telescope mounted perpendicularly to the shock-tunnel nozzle centerline. The telescope permits us to align the laser spot at the nozzle centerline. The laser beam is focused inside the test section through a focusing lens installed in this telescope. A 2-in.-diam NaCl plane-convex lens with a focal distance of 130 mm was used. To make the dimensions of the optic beam compatible with the effective lens area, an optical arrangement was conceived to direct the beam from the laser to the test section. This assembly uses two 2-in.-diam flat mirrors and a 3-m focal-length concave mirror (3-in. diameter) and allows all the energy of the laser to be collected by the lens.

A multichannel time-delay generator synchronized all the equipment used in the experiment (laser, data acquisition system, and schlieren system) within the useful shock-tunnel time. The unit was triggered by a Kistler piezoelectric pressure transducer (model 701 A) located immediately upstream of the nozzle entrance (K1 in Fig. 1). In addition to being the trigger reference, this transducer also supplies the reservoir pressure of the nozzle. Two other Kistler 701 A transducers (located 0.495 m apart at the end of the tunnel-driven section; K2 and K3 in Fig. 1) were used to time the incident shock wave.

Two Hamamatsu GE photodiodes (model B1720-02) were used as light sensors to monitor the generation of the laser pulse (capturing the light emitted between the laser electrodes) and the emission of the light source of the schlieren. The acquisition and storage of the data obtained from the photodiodes and the instrumentation attached to the model and at the driven section was made using a Tektronix VX4244, 16 canals, 200-kHz data acquisition system.

The conventional schlieren arrangement was adopted and conceived to illuminate most of the test-section optical windows. The test section has two 8-in.-diam quartz windows with a 190-mm effective vision area. Because of the positions of the optical tables in the laboratory, an auxiliary optical mounting was necessary to redirect the collimated lamp beam to/from the test section and to make it possible to fix the source light at the parabolic-mirror focus, as shown schematically in Fig. 2. The schlieren visualization system is composed of a xenon flash lamp, two parabolic mirrors (8-in. diameter and 64-in. focal length), a knife edge (razor blade), an ultra-high-speed camera (Cordin 550) used to record the events, and an objective lens. The camera has 32 CCDs and can capture at a maximum rate of 2,000,000 frames per second. In this work, the camera was set to operate at 200,000 frames per second. The auxiliary mounting is composed of two flat mirrors (8-in. diameter) used to guide the collimated beam, a focusing lens (3-in. diameter and 15-cm focal length), and a flat mirror, for which the relative positions were fixed in such a way that the lamp image is formed in the parabolic-mirror focus.

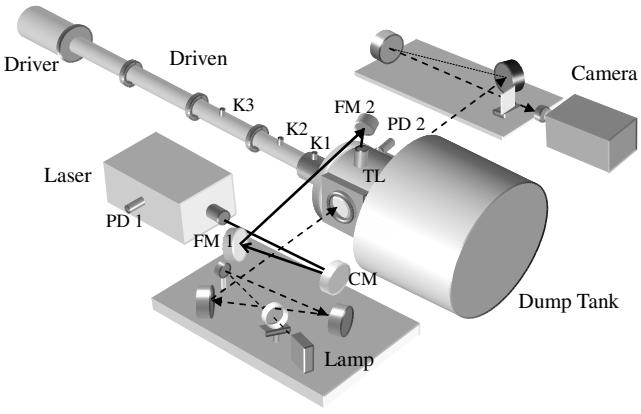

Fig. 1 Schematic of the experimental assembly: laser injection optics, flat mirrors (FM1 and FM2), concave mirror (CM), telescope (TL), pressure transducers (K1, K2, and K3), and photodiodes (PD1 and PD2).

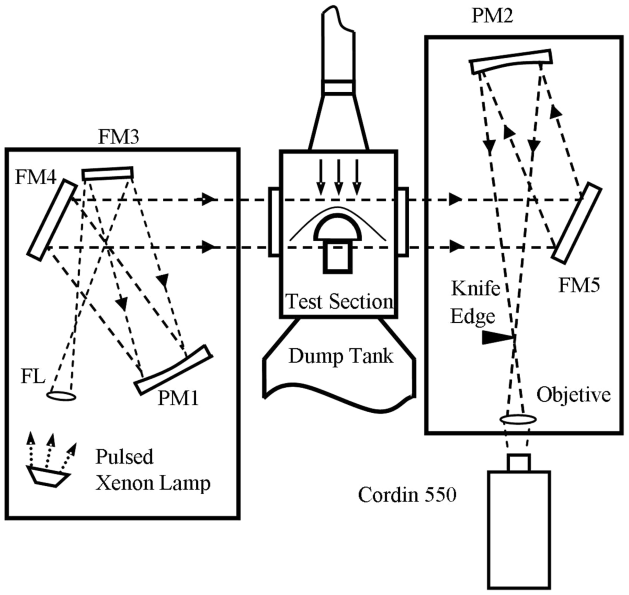

Fig. 2 Schematic of the schlieren layout: flat mirrors (FM), parabolic mirror (PM), and focusing lens (FL).

Table 1 Shock-tunnel test conditions

	Low enthalpy	Medium enthalpy	High enthalpy
Reservoir conditions			
Pressure, bar	29	180	92
Temperature, K	930	1300	4700
Enthalpy, MJ/kg	1.0	1.4	7.5
Freestream conditions			
Pressure, mbar	5	38	29
Temperature, K	85	132	1079
Density, g/m^3	25	101.9	9.33
Mach number	7.3	7.0	5.62

Table 2 CO_2 laser operating conditions

Maximum energy per pulse, J	7.0
Wavelength, μm	10.6
Peak pulse duration, full-width at half-maximum, ns	120
Maximum peak power, MW	30
Total pulse duration, μs	4
Gas mixture	16%CO_2:16%N_2:68%He

III. Experimental Results

A hemispherical model (27.5-mm radius) made of stainless steel was installed in the test section of a hypersonic shock tunnel. It was equipped with a pressure transducer (PCB 112A22) installed inside a recessed-mounting hole (as recommended by the manufacturer) at the stagnation point, to register the impact pressure. The experiments were performed with the model positioned 10.7 and 7 cm downstream of the laser focal region. The laser beam was injected into the tunnel test section perpendicularly to the hypersonic flow, as seen in Fig. 3, in which the model was positioned 7 cm downstream of the focal region.

The tests were conducted at high-, medium-, and low-enthalpy conditions. The nominal shock-tunnel conditions and laser conditions are presented in Table 1 and Table 2, respectively.

The time history of the laser energy addition was recorded by the schlieren system. The ultra-high-speed Cordin 550 camera was set to 200,000 frames per second to permit observation of the evolution of the energy-addition process: the bow shock established by the hypersonic flow, the laser-plasma ignition, the drag and expansion of the laser-induced plasma and laser-induced shock wave (LSW), the interaction between these and the model, and the reconstitution of the bow shock wave on the model. The trigger system allows the selection of the desirable instant of the laser-beam injection.

Excellent results furnished by the schlieren technique were obtained in the experiments. The photograph sequence presented in Fig. 4 shows the time evolution of laser-plasma energy addition at the medium-enthalpy condition (5.4-J laser energy with the model positioned 7 cm downstream of the laser focal region). At the frame rate selected for the experiment (200,000 frames per second), the interval between successive frames is 5 μs and exposure time is 4 μs. At this condition, a total time of 160 μs is registered by the camera, but for convenience, only 100 μs of the time history is shown in figure. Regarding the images obtained in this paper with the schlieren technique, the presence of dark spots (at fixed positions) in the photographs is worth commenting on. The windows of the tunnel test section have marks caused by diaphragm-debris impact and these marks appear as the static black spots in the schlieren photograph.

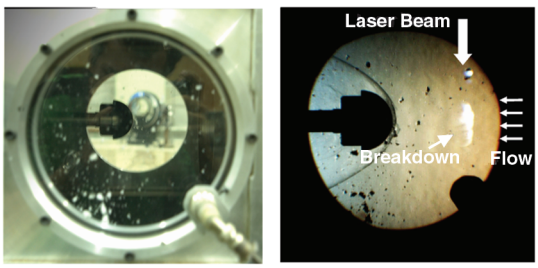

Fig. 3 Hemispherical model positioned 7 cm downstream of the laser focal spot, laser-beam injection perpendicular to Mach 7 hypersonic flow.

Great care was taken to synchronize the laser trigger after the establishment of the flow on the model with the bow shock wave formation, and to confirm these conditions, the camera was set to capture three photographs (instants 0, 5, and 10 μs, not shown in Fig. 4) before the laser injection. In this experiment, the gas breakdown occurred in three distinct regions along the focal region of the laser. The plasma shape varies from one experiment to another due to the presence of dust and aerosol contaminants in the flow, both of which decrease the gas-breakdown threshold [23–26], causing fluctuations of the plasma distribution inside the focal region. As previously mentioned, the laser beam is injected perpendicularly to the flow, with the focal zone extended in a cylindrical region, as can be seen by the plasma brightness extension in the first and second frames in Fig. 4.

The tear-drop shape (inverted because the laser-beam injection is from top to bottom) was the more usual shape obtained for the laser-induced breakdown. However, in several experiments, the breakdown is generated in more than one region, as in the case shown in Fig. 4; as the time elapses, the plasma expands and forms a single surface.

The laser-beam injection is shown at the instant of 15 μs, and the expansion of the shock wave produced by laser generated hot plasma and the drag of the plasma core are shown in the interval range from 15 to 45 μs. After this interval, the disturbance caused by the interaction with the model can be visualized. The laser-supported directed-energy-air-spike effect can be observed from 50 to 115 μs, and the photograph set shows the mitigation of the bow shock wave under the influence of energy addition. At the stagnation point, the frames reveal the effects of the energy addition lasting at least from 50 until 100 μs, and over the total surface of the hemisphere, the effects go beyond the last frame shown in the Fig. 4, occurring at the instant of 135 μs. Figure 5 shows this instant and two subsequent instants (145 and 155 μs) and, for comparison, the instant of 0 μs. The complete recovery of the bow shock produced by the undisturbed hypersonic flow over the model seems to occur only at the instant of 155 μs, because, as shown in the photographs, it is possible to visualize the Prandtl–Meyer expansion in the rear part of the model in the two first frames.

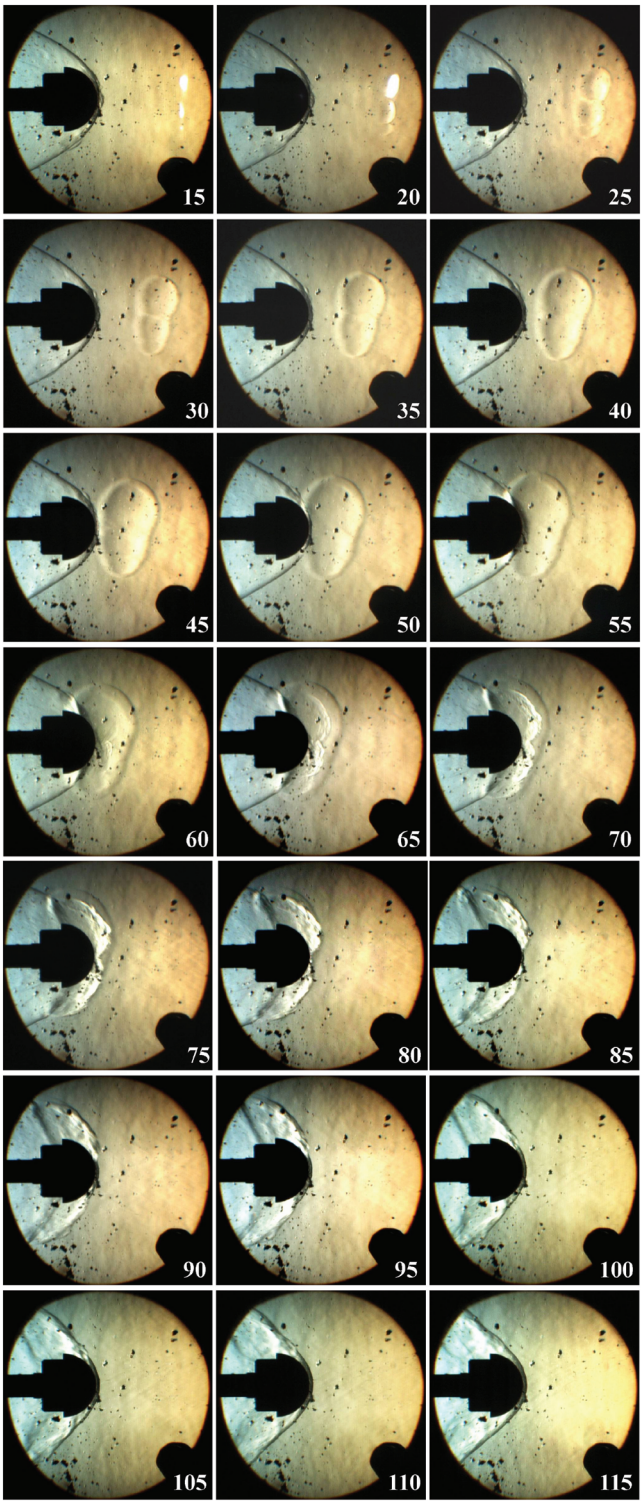

Fig. 4 Schlieren visualization of the bow shock mitigation by laser-plasma energy addition with an interval between frames of 5 μs; laser beam was focused 7 cm upstream of the model; medium-enthalpy condition.

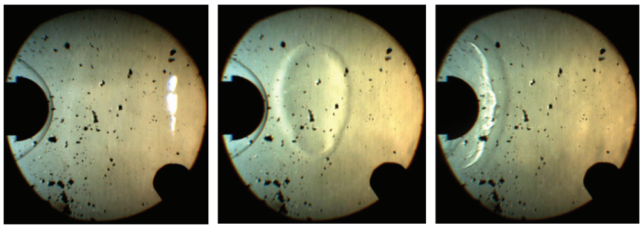

Fig. 6 Laser-plasma energy addition with the model positioned 10.7 cm from breakdown; time interval between frames of 35 μs; medium enthalpy; laser energy 7 J.

To facilitate image analyses, a software program was developed in Visual Basic language, with which the real positions or dimensions in the photographs can be obtained. Thus, using the program, the photograph-set analyses reveal that the hot-gas bubble is dragged by the hypersonic flow at a speed of 1.6 km/s. Using freestream temperature, Mach 7 is obtained for the drag motion, which is coherent with the nominal Mach obtained in the experiment.

The effect of energy addition with the model at 10.7 cm downstream of breakdown is shown in Fig. 6, in which three images (from 32 obtained in the experiment) were selected. The figure shows the breakdown generation and bow shock wave on the model, the hot-gas and LSW expansion, and the bow shock wave mitigation.

The impact pressure at the model centerline was also measured, revealing a pressure drop during that time interval, as shown in Fig. 7. This figure shows the voltage response of the piezoelectric pressure sensor and the signal of laser glow discharge captured by a photodiode. It is important to note that the photodiode does not measure the laser-pulse shape, but gives the instant of laser-pulse generation as reference.

The same behavior of the laser energy addition to hypersonic flow over the impact pressure was obtained in all experiments. To obtain a better insight into the pressure reduction, Fig. 8 presents the results of three experiments attained at the medium-enthalpy condition with the model installed 10.7 cm downstream of the laser focal point. Two of these experiments were performed with laser injection (5.3 and 7.0 J), and to improve the analysis, the pressure signal acquired without laser was incorporated.

Despite the fact that the signal noise has the same frequency as the pressure reduction associated with tunnel operation, the relevant feature is that the valley in the signal was always reproduced at a fixed delay after the laser firing, differently from the random-noise behavior. Comparing the two pressure signals obtained with laser injection, it is noted that the energy difference between these experiments is not large enough to produce a significant change in their behavior, but on the other hand, the three curves shown in Fig. 8 strengthen the reproducibility of the tunnel operation, as well as the pressure drop obtained by laser energy addition.

Experiments at the high-enthalpy condition were also conducted and the results of two of then are shown in Fig. 9 with the model 10.7 cm downstream of the breakdown and laser energy of 6.8 J and 6.0 J, upper/down curve, respectively The impact pressure measured at the high-enthalpy condition is less noisy than the signal obtained at medium enthalpy, as observed by comparing Figs. 8 and 9. If, on one hand, the high-enthalpy condition furnishes a less noisy signal, then on the other hand, the image resolution in the schlieren technique is reduced, due to the lower flow density in this condition. Therefore,

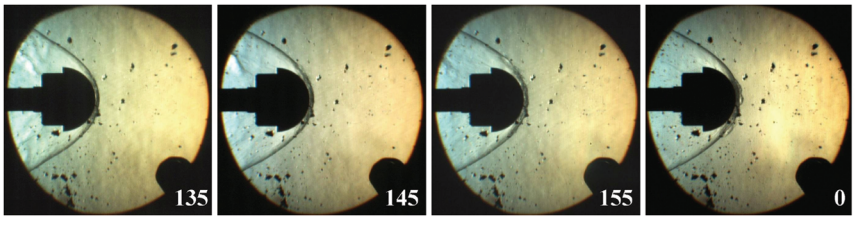

Fig. 5 Photographs showing the instants of 135, 145, 155, and 0 μs.

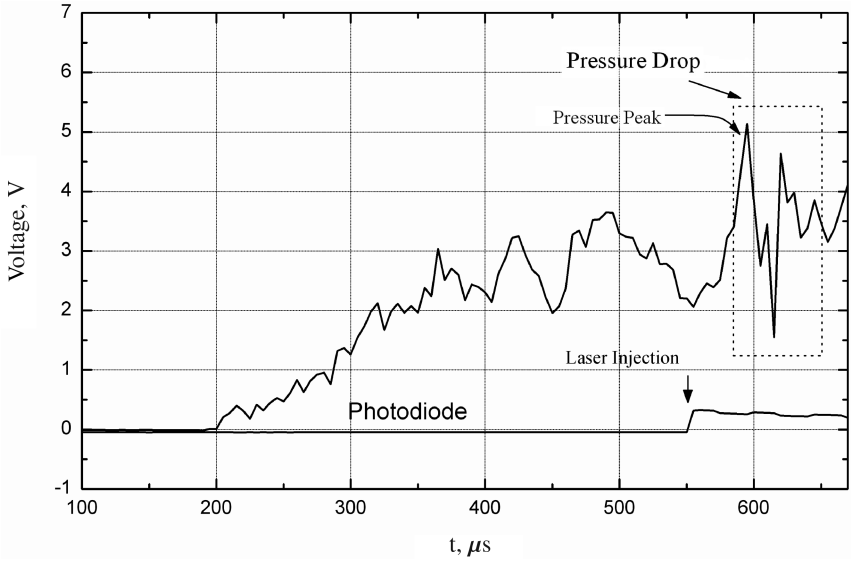

Fig. 7 Impact pressure signal associated with experiment of Fig. 4 showing the pressure drop imposed by the laser energy addition.

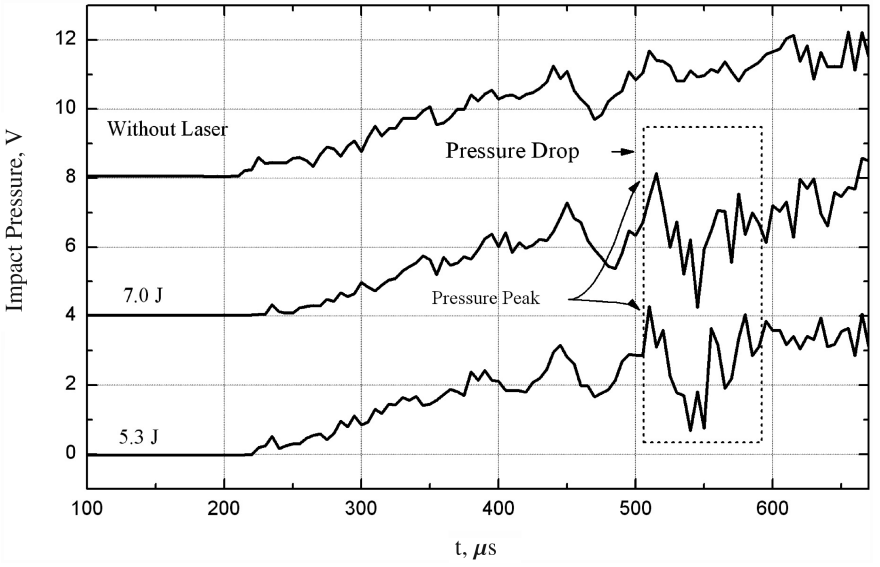

Fig. 8 Impact pressure at the model and pressure drop imposed by laser energy addition (5.3 and 7.0 J) and pressure signal without laser; experiments performed at medium enthalpy with the model 10.7 cm far from breakdown.

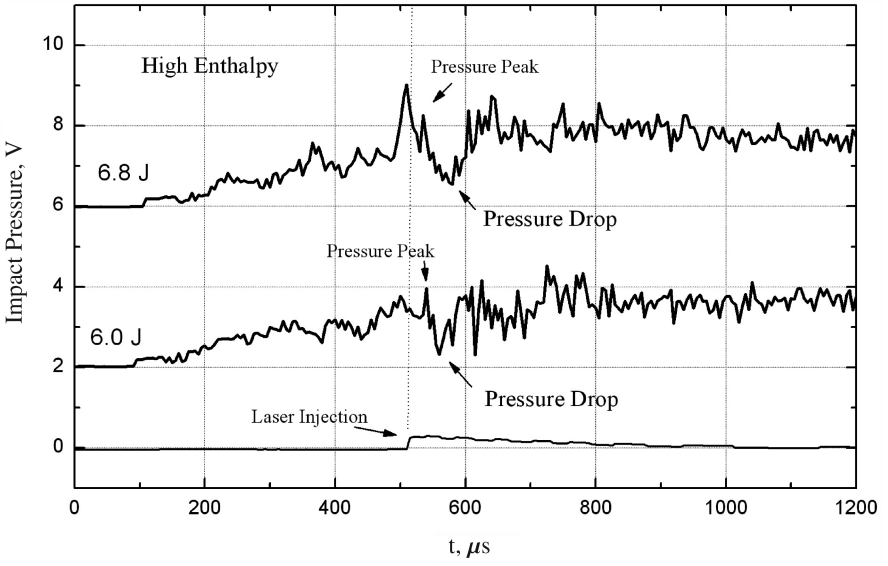

Fig. 9 Impact pressure at the model and pressure drop imposed by laser energy addition (6.8 and 6.0 J). Experiments performed at high enthalpy with model 10.7 cm far from breakdown.

the schlieren sensibility and the camera gain must be improved when acquiring images in this condition.

The range of the pressure drop obtained in our experimental conditions stayed between 30 and 60%, and these values are in agreement with results published in the literature for supersonic and hypersonic flows [9,27–29]. The time duration of the pressure drop at the stagnation point, obtained from the impact pressure signal, furnished the average value of 70 μs. A good correlation between this signal and images displayed by the schlieren technique was obtained in all experiments. The perturbation caused by laser energy addition in these experiments lasts about 100 μs. As mentioned earlier, this value was estimated through the observation of the bow shock recovery time at the rear part of the model. The duration of the pressure drop under the influence of energy addition in our experiments could be larger if the laser were injected parallel to the flow, because (as seen in Fig. 4) the core shape is an ellipsoid in which the minor radius is at about half the major radius at the moment of impact with the model; therefore, a duration two times larger can be expected with this change. The laser-beam injection in this configuration will be the subject of future research.

The schlieren pictures obtained in the experiments also show that the hot gas (core) is still expanding when it collides with the model, as observed in its time evolution between instants of 15 (breakdown generation) and 50 μs (impact on the model), therefore revealing that the gas temperature and pressure inside the core is not in equilibrium with the surrounding.

Another aspect revealed by the pressure signals is shock–shock interaction [30,31] detected by the pressure transducer at the moment the LSW reaches the stagnation point. This is caused by the penetration of the LSW into the bow shock wave. As shown in the curves of Figs. 7–9, the pressure drop is preceded by a peak of pressure increase.

The detachment between expansion of the hot gas (core) and the LSW can be inferred from Fig. 4. When the high-power laser pulse is delivered to the gas, the breakdown occurs, the hot plasma expands quickly, and the laser-supported detonation wave is established. After the laser pulse ends, the detonation mechanism ceases and the expansion rate decreases. The hot gas starts to expand more slowly than the LSW, increasing the gap between the core contour and the LSW, as observed in the frame sequence. The experiments described in this paper were directed to visualize the effect of the energy addition to the flow, including the interaction with the model. The frame rate adequate to this goal is not high enough to make visualization of the laser-supported detonation wave possible. This study will be realized in the future, using the maximum speed of the Cordin 550 camera (2,000,000 frames per second).

The detachments that occurred in two different experiments are also seen in Fig. 10. In these experiments, the breakdown occurred at the instant of 15 μs, and the instants of 45 and 70 μs were selected to show the time behavior. The runs were conducted at medium-enthalpy (upper images) and low-enthalpy (lower images) conditions. The figure also shows the gas compression near the core edges, as indicated by the white arrows. When the core reaches the model, a compression wave propagates in the direction of the core edges and a layer of compressed gas is generated near the core surface.

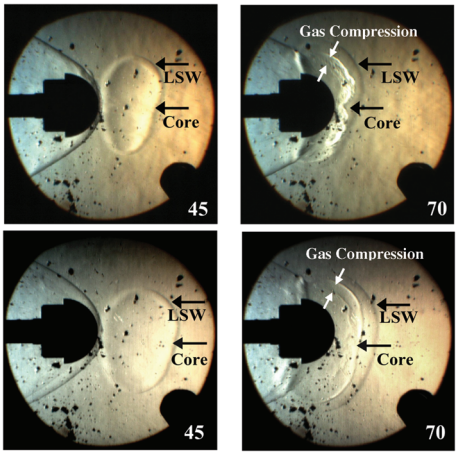

Fig. 10 Schlieren visualization of the expansion of the LSW and the core for instants of 45 and 70 μs for two experiments conducted at medium (upper) and low enthalpy.

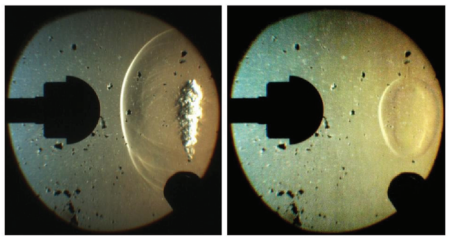

a) b)

Fig. 11 Schlieren visualization of the laser-induced breakdown in quiescent gas: a) 1 atm and b) 80 mbar.

The enthalpy conditions have a great influence on the threshold of the laser-induced breakdown. At our experimental conditions, in medium- and high-enthalpy conditions, the breakdown was generated in 100% of the experiments, whereas in the low-enthalpy condition, the breakdown occurred only in 40% of the runs. The same laser settings and driven gas were used in the experiments. At the present moment, we still do not have a theoretical explanation to justify the higher threshold observed in the low-enthalpy condition.

The schlieren images also demonstrated that the internal structure of the core changes with pressure. Before each experiment, both the optical alignment of schlieren and laser-beam injection were tested. This procedure was conducted at ambient pressure. The breakdown generated in this condition discloses a complex inner-core structure that survives for a long time (milliseconds). On the other hand, for the freestream pressure levels discussed in the present paper, the core was homogeneous in all experiments. For comparison, Fig. 11 shows two schlieren pictures in which the effects of pressure can be visualized. In Fig. 11a, the breakdown was generated in quiescent gas at 1 atm, and in Fig. 11b, the breakdown was at 80 mbar. The elapsed time after breakdown was 120 μs in Fig. 11a and 105 μs in Fig. 11b.

IV. Conclusions

The schlieren technique is a powerful tool to analyze experiments in the hypervelocity field because it is inexpensive, nonintrusive, and easy to align. In studies of energy addition to the flow, it furnishes images with a wealth of details about the dynamics of the phenomena and it can be used to determine laser parameters such as the energy and repetition rate necessary to maintain a desirable change in the shock wave profile ahead of a vehicle. The schlieren technique also makes it possible to study the surface profiles that are more adequate to hypersonic vehicle design. The possible benefits of this kind of laser application (such as the drag and heat transfer reduction to vehicles, maneuver control, and reduction of temperature of parts of vehicle surfaces) can be at least partially analyzed with this technique. The images obtained in this paper using this technique are a good example of its power. The time history of the energy addition to hypersonic flow by laser-induced plasma generation and its effects over a hemispherical model can be registered in photographs. In this way, the breakdown generation, the core and the laser-induced shock wave expansions, the interaction of both with the model, and the recovering of the bow shock wave are recorded and the images provide details of inner structure of the flowfield in this interaction.

Acknowledgments

The authors gratefully acknowledge Alberto M. dos Santos, Chief of the Department of Aerothermodynamics and Hypersonics at the Institute for Advanced Studies, for his comments and suggestions for

this work. The authors would like to thank David R. Pinto, Douglas D. Glansmann, Francisco R. de Jesus, and Douglas S. Silveira for help in the operation of the tunnel.

References

[1] Toro, P. G. P., Nagamatsu, H. T., Minucci, M. A. S., and Myrabo, L. N., "Experimental Pressure Investigation of a 'Directed-Energy Air Spike' Inlet at Mach 10," AIAA Paper 99-2843, June 1999.

[2] Toro, P. G. P., Nagamatsu, H. T., Myrabo, L. N., and Minucci, M. A. S., "Experimental Heat Transfer Investigation of a 'Directed-Energy Air Spike' Inlet at Mach 10," AIAA Paper 99-2844, June 1999.

[3] Minucci, M. A. S., Bracken, R. M., Myrabo, L. N., Nagamatsu, H. T., and Shanahan, K. J., "Experimental Investigation of an Electric Arc Simulated 'Air-Spike' in Hypersonic Flow," AIAA Paper 00-0715, Jan. 2000.

[4] Bracken, R. M., Myrabo, L. N., Nagamatsu, H. T., Meloney, E. D., and Shneider, M. N., "Experimental Investigation of an Electric Arc Air-Spike with and Without Blunt Body in Hypersonic Flow," AIAA Paper 2001-0796, Jan. 2001.

[5] Leonov, S. B., and Bityurin, V. A., "Hypersonic/Supersonic Flow Control by Electro-Discharge Plasma Application," 11th AIAA/AAAF International Symposium Space Planes and Hypersonic Systems and Technologies, Orleans, France, AIAA Paper 2002-5209, 2002.

[6] Minucci, M. A. S., Toro, P. G. P., Chanes, J. B., Jr., Ramos, A. G., Pereira, A. L., Nagamatsu, H. T., and Myrabo, L. N., "Investigation of a Laser-Supported Directed-Energy 'Air Spike' in Hypersonic Flow," *Journal of Spacecraft and Rockets*, Vol. 40, No. 1, 2003, pp. 133–136.

[7] Takaki, R., and Liou, M.-S., "Parametric Study of Heat Release Preceding a Blunt Body in Hypersonic Flow," *AIAA Journal*, Vol. 40, No. 3, Mar. 2002, pp. 501–509.

[8] Minucci, M. A. S., Toro, P. G. P., Oliveira, A. C., Ramos, A. G., Chanes, J. B., Jr., Pereira, A. L., Nagamatsu, H. T., and Myrabo, L. N., "Laser-Supported Directed-Energy 'Air Spike' in Hypersonic Flow," *Journal of Spacecraft and Rockets*, Vol. 42, No. 1, Jan.–Feb. 2005, pp. 51–57.
doi:10.2514/1.2676

[9] Adelgren, R. G., Elliott, G. S., Knight, D. D., Zheltovodov, A. A., and Beutner, T. J., "Energy Deposition in Supersonic Flows," 39th AIAA Aerospace Sciences Meeting and Exhibit, Reno, NV, AIAA 2001-0885, Jan. 2001.

[10] Minucci, M. A. S., Toro, P. G. P., Oliveira, A.C., Chanes, J. B., Jr., Ramos, A. G., Nagamatsu, H. T., and Myrabo, L. N., "Multi Laser Pulse Investigation of the DEAS Concept in Hypersonic Flow," *2nd International Symposium on Beamed Energy Propulsion*, edited by K. Komurasaki, American Inst. of Physics, Woodbury, NY, 2003, pp. 480–492.

[11] Kolesnichenko, Y. F., Brovkin, V. G., Azarova, O. A., Grudnitsky, V. G., Lashkov, V. A., and Mashek, I. Ch., "Microwave Energy Release Regimes for Drag Reduction in Supersonic Flows," AIAA Paper 2002-0353, 2002.

[12] Kolesnichenko, Y. F., Brovkin, V. G., Azarova, O. A., Grudnitsky, V. G., Lashkov, V. A., and Mashek, I. Ch., "MW Energy Deposition for Aerodynamic Application," 41st AIAA Aerospace Sciences Meeting and Exhibit, Reno, NV, AIAA Paper 2003-0361, Jan. 2003.

[13] Tretyakov, P. K., Grachev, G. P., Ivanchenko, A. I., Krainev, V. L., Ponomarenko, A. G., and Tishchenko, V. N., "Stabilization of the Optical Discharge in a Supersonic Argon Flow," *Physics-Doklady*, Vol. 39, No. 6, 1994, pp. 415–416; translated from *Doklady Akademii Nauk*, Vol. 336, No. 4, 1994, pp. 466–467.

[14] Myrabo, L. N., and Raizer, Y., "Laser-induced Air Spike for Advanced Transatmospheric Vehicles," AIAA Paper 94-245, 1994.

[15] Hill, G. A., James, D. J., and Ramsden, S. A., "Breakdown Thresholds in Rare and Molecular Gases Using Pulsed 10.6 μm Radiation," *Journal of Physics D: Applied Physics*, Vol. 5, No. 11, Nov. 1972, pp. L97–L99.
doi:10.1088/0022-3727/5/11/101

[16] Raizer, Y., "Breakdown and Heating of Gases Under the Influence of a Laser Beam," *Soviet Physics, Uspekhi*, Vol. 8, No. 5, 1966, pp. 650–673.
doi:10.1070/PU1966v008n05ABEH003027

[17] Raizer, Y., *Gas Discharge Physics*, 2nd ed., Springer–Verlag, New York, 1997.

[18] Mohamed, Gad-El-Hak, "Splendor of Fluids in Motion," *Progress in Aerospace Sciences*, Vol. 29, No. 2, 1992, pp. 81–123.
doi:10.1016/0376-0421(92)90004-2

[19] Liepmann, H. W., and Roshko, A., *Elements of Gasdynamics*, Wiley, New York, 1967.

[20] Nascimento, M. A. C., Minucci, M. A. S., Ramos, A. G., Changes, J. B., Jr., and Nagamatsu, H. T., "Hypersonic Gaseous Piston Shock Tunnel: Numerical and Experimental Results," 36th Aerospace Sciences Meeting and Exhibit, Reno, NV, AIAA Paper 98-0548, Jan. 1998.

[21] Nascimento, M. A. C., "Gaseous Piston Effect in Shock Tube/Tunnel When Operating in the Equilibrium Interface Condition," Ph.D. Dissertation, Div. de Engenharia Aeronáutica, Inst. Tecnológico de Aeronáutica, São José dos Campos, Brazil, Oct. 1997.

[22] Watanuki, J. T., Oliva, J. L. S., Lobo, M. F. G., and Rodrigues, N. A. S., "Laser de CO2-Híbrido com Célula de Baixa Pressão Pulsada," *Revista de Física Aplicada e Instrumentação*, Vol. 3, No. 3, 1988, pp. 207–216 (in Portuguese).

[23] Morgan, C. G., "Laser-Induced Breakdown of Gases," *Reports on Progress in Physics*, Vol. 38, No. 5, May 1975, pp. 621–665.
doi:10.1088/0034-4885/38/5/002

[24] Lencioni, D. E., "The Effect of Dust on 10.6 μm Laser-Induced Air Breakdown," *Applied Physics Letters*, Vol. 23, No. 1, July 1973, pp. 12–14.
doi:10.1063/1.1654718

[25] Canavan, G. H., and Nielsen, P. E., "Focal Spot Size Dependence of Gas Breakdown Induced by Particulate Ionization," *Applied Physics Letters*, Vol. 22, No. 8, Apr. 1973, pp. 409–410.
doi:10.1063/1.1654693

[26] Smith, D. C., "Laser Induced Gas Breakdown and Plasma Interaction," 38th Aerospace Sciences Meeting and Exhibit, Reno, NV, AIAA Paper 2000-0716, Jan. 2000.

[27] Kandala, R., and Candler, G. V., "Numerical Studies of Laser-Induced Energy Deposition for Supersonic Flow Control," *AIAA Journal*, Vol. 42, No. 11, Nov. 2004, pp. 2266–2275.
doi:10.2514/1.6817

[28] Zaidi, S. H., Shneider, M. N., and Miles, R. B., "Shock-Wave Mitigation Through Off-Body Pulsed Energy Deposition," *AIAA Journal*, Vol. 42, No. 2, Feb. 2004, pp. 326–331.
doi:10.2514/1.9097

[29] Knight, D., Kuchinskiy, V., Kuranov, A., and Sheikin, E., "Survey of Aerodynamic Flow Control at High Speed by Energy Deposition," 41st AIAA Aerospace Sciences Meeting and Exhibit, Reno, NV, AIAA Paper 2003-0525, Jan. 2003.

[30] Miller, H. R., "Shock-on-Shock Simulation and Hypervelocity Flow Measurements with Spark-Discharge Blast Wave," AIAA Paper 66-773, 1966.

[31] Adelgren, R. G., Hong, Y., Elliott, G. S., Knight, D. D., Beutner, T. J., and Zheltovodov, A. A., "Control of Edney IV Interaction by Pulsed Laser Energy Deposition," *AIAA Journal*, Vol. 43, No. 2, Feb. 2005, pp. 256–269.
doi:10.2514/1.7036

I. Boyd
Associate Editor